Energetics of Denaturation and *m* Values of Staphylococcal Nuclease Mutants†

John H. Carra and Peter L. Privalov*

Department of Biology and Biocalorimetric Center, The Johns Hopkins University, Baltimore, Maryland 21218

Received September 27, 1994; Revised Manuscript Received November 8, 1994®

ABSTRACT: In a continuation of an earlier study [Carra, J., Anderson, E., & Privalov, P. (1994) *Biochemistry 33,* 10842−10850], we used differential scanning calorimetry to measure the enthalpy and heat capacity changes of denaturation for 11 mutant forms of staphylococcal nuclease, including the triple mutant [V66L+G88V+G79S]. Several mutant proteins with m^- characteristics of guanidinium chloride denaturation were found to denature via a three-state mechanism with increasing temperature. Enthalpy changes for the transitions from the native to intermediate and from the intermediate to denatured states were determined. In the case of the triple mutant, the enthalpy of the second endothermic transition is greater than that of the first. Observation of this second transition provides an explanation for the previously reported large changes in the ΔH of denaturation for the triple mutant versus wild-type nuclease. The sequence specificity of structure in the intermediate state is discussed with relevance to *m* values of guanidinium chloride denaturation. The enthalpic level of the intermediate state depends upon the amino acid sequence, suggesting that stabilizing mutations can increase the extent or cohesion of structure present in the intermediate.

Staphylococcal nuclease is a small protein (149 amino acids) widely used as a model system for the study of protein folding. Previously, our laboratory and other laboratories have studied the thermodynamics of denaturation of staphylococcal nuclease and its mutant forms using microcalorimetry, or fluorescence measurements (Calderon et al., 1985; Griko et al., 1988, 1994b; Shortle et al., 1988; Gittis et al., 1993; Tanaka et al., 1993; Carra et al., 1994a,c; Wu et al., 1994; Xie et al., 1994).

The studies of Shortle et al. (1988) and Tanaka et al. (1993) found large differences in the enthalpy change of denaturation of certain mutant proteins versus wild-type nuclease. In an extreme case, the enthalpy change of the triple mutant [V66L+G88V+G79S] was found using fluorescence by Shortle et al. (1988) to be 156 kJ mol^{-1} less than that of the wild-type protein at 47.9 °C. Tanaka et al. (1993), using calorimetry, found it to be 218 kJ mol^{-1} less than the wild-type ΔH of 309 kJ mol^{-1} at 51.4 °C. These large differences in ΔH seemed to be incompatible with the notion that the enthalpy change of protein denaturation is proportional to the surface areas exposed to solvent upon unfolding (Makhatadze & Privalov, 1993; Privalov & Makhatadze, 1993), leading to skepticism about the possibility of relating information on protein structure to thermodynamic quantities (Sturtevant, 1994).

In an earlier paper (Carra et al., 1994c), we found that the denaturation of some mutant nucleases is a three-state process, including an intermediate which we call the I-state. Using differential scanning calorimetry, we observed two distinct endothermic transitions, which we ascribed to the individual melting of subdomains of the protein. Changes in circular dichroism at 222 nm or fluorescence from tryptophan 140 monitor mainly the first transition and miss the second. The enthalpy and Gibbs free energy changes of the second transition can therefore easily be neglected if this denaturation is considered only as a two-state reaction, as was done in previous studies.

In this work, we apply microcalorimetry to 11 substitution mutants of staphylococcal nuclease. The positions of these mutations in the protein structure are shown in Figure 1. We find that the second endothermic transition of the triple mutant protein [V66L+G88V+G79S] has a large enough enthalpy change to account for most or all of the missing enthalpy reported. The enthalpy changes associated with melting of the intermediate states of different mutant proteins can vary by 2-fold, suggesting that the I-state encompasses forms of differing structural content.

These findings about thermal denaturation also have relevance to the process of guanidinium chloride induced denaturation. Mutant nucleases which denature over a broader range of guanidinium chloride concentration than the wild-type protein are described as m^-, while conversely mutants which denature over a narrower range are m^+ (Shortle & Meeker, 1986). Our present study of a larger number of mutant nucleases confirms a correlation between the m^- characteristic of guanidinium chloride denaturation and the presence of the thermal intermediate. We also apply the transverse urea gradient gel electrophoresis method of Creighton (1979) to compare the denaturation of m^- and m^+ mutants.

EXPERIMENTAL PROCEDURES

Protein Preparation. Escherichia coli strains overproducing staphylococcal nuclease A (Foggi strain), and mutants thereof, were generously supplied by the laboratory of Dr. David Shortle. Proteins were purified and quantified as previously described (Carra et al., 1994a,b). In the case of the G88W mutant, which has an additional tryptophan residue, the method of Gill and von Hippel (1989) was used

† This work was supported by NIH Grant GM 48036 and NSF Grant MCB 9118687.

* To whom correspondence should be addressed. Telephone: 410-516-6532. Fax: 410-516-5213.

® Abstract published in *Advance ACS Abstracts,* January 1, 1995.

0006-2960/95/0434-2034$09.00/0

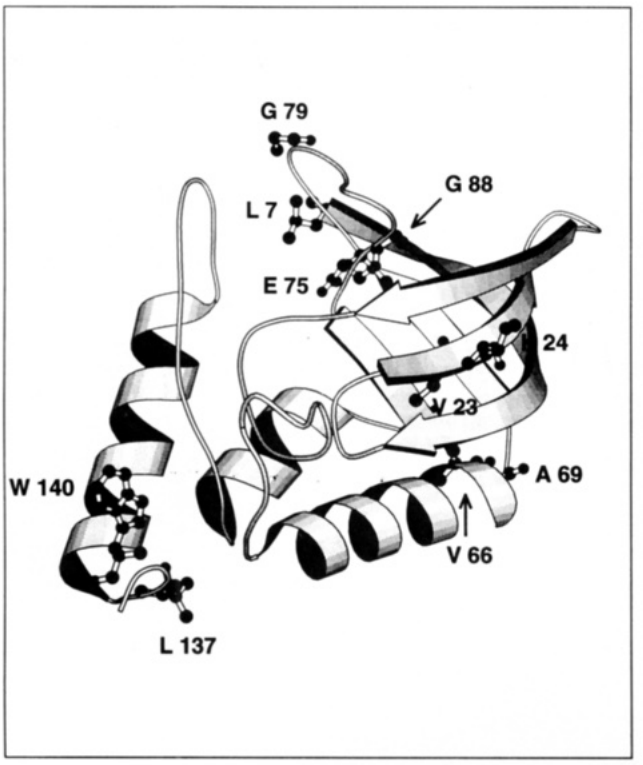

FIGURE 1: Ribbon drawing of the structure of Ca^{2+} and pdTp-liganded staphylococcal nuclease (Loll & Lattman, 1989). The figure was drawn using the program MOLSCRIPT (Kraulis, 1991), with coordinates from the Brookhaven Protein Data Bank (1snc.pdb). The ligands, and the disordered amino acids 1−6 and 141−149, are not shown. Leucine 7, valine 23, lysine 24, valine 66, alanine 69, glutamate 75, glycine 79, glycine 88, leucine 137, and tryptophan 140 are shown in a ball-and-stick presentation.

to obtain an extinction coefficient of 1.29 cm^{-1} for a 1 mg mL^{-1} protein solution.

Microcalorimetry, Circular Dichroism, and Fluorescence Measurements. All these techniques were done as previously described (Carra et al., 1994c).

Transverse Urea Gradient Gels. These were prepared using a modification of the method of Creighton (1979). Polyacrylamide gels were poured containing either a 0−4 or 0−6 M urea gradient in an 18 × 18 × 0.15 cm slab. An improvised gradient maker was used consisting of two 50 mL plastic tubes connected with tubing to each other and to a peristaltic pump. The pump dripped the gel mixture down into a glass plate sandwich held sideways relative to the electrophoresis direction, with the heavier urea-containing solution going first. An acrylamide stock solution of 30/0.8% [acrylamide/bis(acrylamide)] was diluted to 7.5% acrylamide in the 0 M urea gel mixture, 6.2% in the 4 M urea mixture, and 5.5% in the 6 M mixture, in order to compensate for reduced protein mobility at high urea concentrations due to greater viscosity (Creighton, 1979). The buffer in the gel and in the reservoirs was 50 mM Tris−acetate, 1 mM EDTA, pH 7.0. Polymerization was initiated with low concentrations of ammonium persulfate and TEMED. For each protein, 200 μL of a 1 mg mL^{-1} protein solution in water containing Pyronin Y tracking dye was loaded across the top of the gel. Electrophoresis was performed toward the anode for approximately 4.5 h at 105 V in a vertical apparatus. The temperature of the gel was only slightly warmer than room temperature and was not regulated.

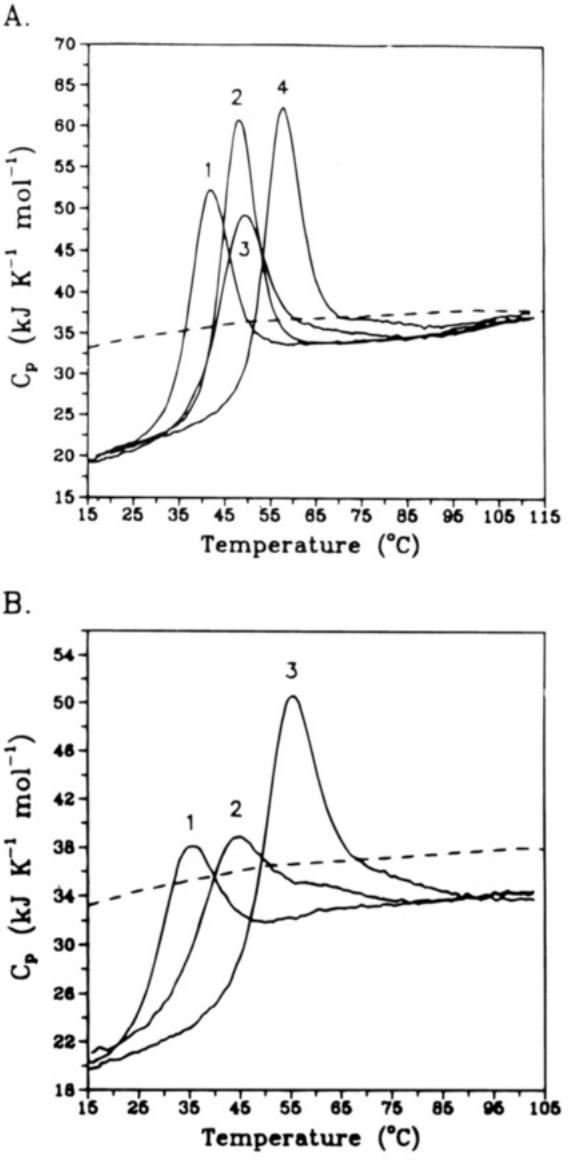

FIGURE 2: Differential scanning calorimetry (DSC) on mutant nuclease proteins. Buffer components are given in Table 1. (A) At pH 7.0: (1) V23A; (2) K24G; (3) E75A; (4) G88W. The dashed line is the calculated heat capacity of a hypothetical fully unfolded nuclease determined according to Makhatadze and Privalov (1990). (B) At pH 5.0: (1) A69T; (2) V23F; (3− G88W.

RESULTS

Figure 2A shows differential scanning calorimetry curves done at pH 7.0 on four mutant nuclease proteins: V23A, K24G, E75A, and G88W. The calculated heat capacity of a fully unfolded nuclease (Makhatadze & Privalov, 1990) is given as a reference (dashed line). The V23A and K24G proteins melt with one peak apparent. After this peak, the heat capacity function is fairly flat. Deconvolution and fitting of the curves (Biltonen & Freire, 1978; Privalov & Potekhin, 1986) indicate that the melting of these proteins is a two-state process; i.e., any equilibrium intermediates are present only as a vanishingly small fraction of the population of molecules. Table 1 gives the T_t,[1] ΔH, and ΔS values of the denaturation reactions.

[1] Abbreviations: C_p, heat capacity; $\langle C_p \rangle$, excess heat capacity; DSC, differential scanning calorimetry; T_t, transition temperature; CD, circular dichroism; pdTp, thymidine 3′,5′-bisphosphate.

Table 1: Calorimetric Results of Mutant Nuclease Denaturation

mutant	T_t[a] (peak 1)	T_t[a] (peak 2)	ΔH_{cal}[b] (total)	ΔH_{fit}[b] (peak 1)	ΔH_{fit}[b] (peak 2)	ΔS[c] (peak 1)	ΔS[c] (peak 2)	fit error[d]
				pH 7.0[e]				
wild-type	54.1		324	356		0.99		0.044
L7A	50.9		310	313		0.96		0.028
V23A	41.6		276	278		0.88		0.016
V23F[f]	47.8							
K24G	47.9		321	327		1.00		0.016
A69T	40.5		260	282		0.83		0.039
E75A	48.5	63.3	326	241	82	0.75	0.24	0.020
E75G	38.9	65.8	246	198	73	0.63	0.22	0.020
G79S	49.7	58.5	285	227	70	0.70	0.21	0.018
G88W	58.7	64.4	382	304	87	0.91	0.26	0.017
L137A	45.3		253	268		0.79		0.039
[V66L+G88V+G79S]	57.6	69.1	315	154	165	0.47	0.48	0.007
				pH 5.0[g]				
wild-type	50.8		306	299		0.95		0.016
L7A	47.4		247	247		0.77		0.018
V23A	34.9		183	189		0.60		0.025
V23F	44.0	55.9	230	161	83	0.51	0.25	0.019
K24G	42.6		251	253		0.80		0.010
A69T	34.3		159	186		0.52		0.050
E75A	41.9	57.1	239	148	99	0.47	0.30	0.008
G79S	45.2	60.3	260	184	83	0.58	0.25	0.008
G88W	55.6	66.2	340	244	105	0.74	0.31	0.010
L137A	39.6		155	180		0.50		0.052
[V66L+G88V+G79S]	53.7	68.7	341	146	189	0.45	0.55	0.007
				pH 4.1[h]				
G88W	48.8	55.3	221	149	80	0.46	0.24	0.014
[V66L+G88V+G79S]	41.4	64.9	279	129	161	0.41	0.48	0.011

[a] Transition temperature in degrees centigrade. Errors are ±0.5 K. [b] In kJ mol^{-1}. Errors on enthalpies are approximately ±10%. [c] In kJ K^{-1} mol^{-1}. ΔH_{cal} and not ΔH_{fit} was used to calculate ΔS when there was one transition only. Errors are approximately ±10%. [d] Mean square deviation of the fitted curves. [e] 20 mM sodium phosphate, 100 mM NaCl, and 1 mM EDTA, pH 7.0. [f] Only T_{t1} of V23F could be obtained at pH 7.0, due to aggregation of the denatured protein during the second endotherm. Aggregation was not observed at pH 5.0. [g] 20 mM NaOAc, 100 mM NaCl, and 1 mM EDTA, pH 5.0. [h] 20 mM glycine hydrochloride, 100 mM NaCl, and 1 mM EDTA, pH 4.1.

In contrast, the mutant proteins E75A and G88W show a broad second transition after the major peak. Deconvolution analysis reveals that the melting of these proteins is a three-state process. Unfolding proceeds through an intermediate state, which is distinguished from the final denatured state by a measured enthalpy change (Table 1). We find that both endothermic transitions of mutant nucleases are mostly reversible (Carra et al., 1994c), as long as the sample is not heated above 80 °C.

The absolute heat capacity values of the native and denatured states of all the mutant proteins are the same, within an error of ±2 kJ K^{-1} mol^{-1}. The total ΔC_p values of denaturation of these proteins are therefore equal within error. This result is as should be expected, because the heat capacity changes of denaturation of proteins have been found to be proportional to the surface areas exposed to solvent upon unfolding (Makhatadze & Privalov, 1993, Privalov & Makhatadze, 1993). Single mutations which do not greatly perturb the protein's structure therefore will not produce a measurable difference in the ΔC_p of unfolding.

Figure 2B shows DSC results at pH 5.0 for three proteins: A69T, V23F, and G88W. A69T denatures with one definite peak and only a small suggestion of a second. V23F and G88W, on the other hand, clearly give broad second endotherms. The heat capacity of the final denatured state is lower at pH 5.0 than at pH 7.0, a phenomenon which we have observed before, but which lacks definite explanation (Carra et al., 1993a). The lower heat capacity of the denatured state at lower pH may indicate that the denatured state is incompletely unfolded under acidic conditions, even at 100 °C.

Of the mutant proteins shown in Figure 2, V23A, K24G, and A69T are classified as m^+ with respect to guanidinium chloride induced denaturation, while V23F, E75A, and G88W are m^- (Gittis et al., 1993; Green & Shortle, 1993; Shortle et al., 1990; Shortle & Meeker, 1986). m values from the literature are given in Table 2. The presence of a strong second endotherm in the thermal denaturation of these mutants correlates with the m^- characteristic.

The triple mutant protein [V66L+G88V+G79S] has an m value of 0.51, relative to the wild-type value of 1 (Shortle & Meeker, 1986). This is the lowest m value reported to date for a staphylococcal nuclease mutant. This protein also displays the strongest second endotherm of all the mutant nucleases we have studied. Calorimetry on [V66L+G88V+G79S] protein at pH 7.0 gives an exceptionally broad peak (Figure 3A), which deconvolution reveals to be composed of two underlying endotherms (Figure 3B). The result is well fit to a model of two sequential first-order transitions (Carra et al., 1994c; Privalov & Potekhin, 1986). The second endotherm is slightly larger than the first (Table 1).

With decrease of pH to 4.1, the broad peak found at pH 7.0 divides itself into two well-separated transitions (Figure 3A). The first endotherm is sensitive to pH changes in the region from 7 to 4, while the second endotherm is relatively unaffected (Carra et al., 1994c). Decrease of pH has caused the first transition to move to lower temperatures away from the second transition.

Figure 4 shows the populations of the native, intermediate, and denatured states for [V66L+G88V+G79S] as a function of temperature at pH 4.1, calculated using the calorimetric

Table 2: Comparison of Mutant Enthalpies and Gibbs Free Energies

protein	m[a]	ΔT_t[b]	$\Delta\Delta G$ (GuHCl)[c]	$\Delta\Delta G_{tot}$ (calor)[d]	$\Delta\Delta G_1$[e]	ΔH_{tot}[f]	ΔH_1[g]	$\Delta\Delta H_{tot}$[h]
wild-type	1.0	0	0	0	0	295	295	0
L7A	0.89[i]	−3.2	−6.6[i]	−2.0	−2.0	304	304	9
V23A	1.18[j]	−12.5	−12[j]	−7.2	−7.2	335	335	40
K24G	(m^+)[k]	−6.3		−1.7	−1.7	336	336	41
A69T	1.13[i]	−13.7	−11[i]	−8.7	−8.7	327	327	31
E75A	(m^-)[k]	−5.6		0.3	−7.3	319	250	24
E75G	(m^-)[k]	−15.2		−5.7	−12	322	264	27
G79S	0.82[i]	−4.4	−11[i]	−2.7	−8.4	290	229	−5
G88W	0.66[l]	4.6	−5.1[l]	8.8	0.4	324	251	29
L137A	0.95[j]	−8.7	−9.6[j]	−8.0	−8.0	286	286	−10
[V66L+G88V+79S}	0.51[m]	3.5	−13[m]	3.2	−17	254	108	−42

[a] The m value for denaturation by guanidinium chloride. Data from the literature as cited. [b] The calorimetrically determined difference in transition temperature between a mutant and wild-type protein at pH 7.0. Data are for peak 1 from Table 1. V23F is not included due to aggregation at pH 7.0 (see Table 1 legend). Errors are ±0.5 K. [c] Data from the literature for the difference in Gibbs free energy of unfolding between a mutant and wild-type protein at 20 °C in kJ mol^{-1}, as determined by guanidinium chloride denaturation, assuming a two-state transition. [d] The difference in the total Gibbs free energy of unfolding of a mutant protein versus wild-type, in kJ mol^{-1}, measured calorimetrically at pH 7.0. Results were extrapolated to 20 °C from data in Table 1 using ΔC_p values of 6 ± 1 and 1 ± 1 kJ K^{-1} mol^{-1} for the first and second transitions, respectively. For wild-type, L7A, V23A, K24G, A69T, and L137A proteins, the results were fitted to one transition, ΔC_p was taken as 7 kJ K^{-1} mol^{-1}, and the calorimetric ΔH value was used to calculate ΔG. Errors on Gibbs free energies are estimated at ±2 kJ mol^{-1}. [e] The Gibbs free energy difference at 20 °C between the first endothermic transition of a mutant protein and the total Gibbs free energy of unfolding of the wild-type protein, in kJ mol^{-1}. [f] The extrapolated total enthalpy of unfolding at 50 °C, in kJ mol^{-1}. [g] The extrapolated enthalpy at 50 °C of the first endothermic transition, in kJ mol^{-1}. [h] The difference in total enthalpy of unfolding between a mutant and wild-type protein at 50 °C, in kJ mol^{-1}. [i] Green & Shortle (1993). [j] tShortle et al. (1990). [k] Personal communication from Dr. David Shortle. [l] Gittis et al. (1993). [m] Shortle & Meeker (1986).

data in Table 1 and ΔC_p estimates of 4 and 1 kJ K^{-1} mol^{-1} for the first and second transition, respectively. The intermediate state reaches a maximum of 79% of the population at 54 °C. At pH 7.0, the intermediate state population is calculated to reach a maximum of 58% at 63 °C (not shown), using estimated ΔC_p values of 6 and 1 kJ K^{-1} mol^{-1} for the two transitions, respectively. Figure 4 also shows the fractional changes observed in ellipticity at 222 nm and fluorescence from tryptophan 140. The single transition found by each of these methods occurs in parallel with the transition from the native to intermediate states, as we have observed previously with other mutants (Carra et al., 1994c). This means that energetic parameters calculated from fluorescence or circular dichroism data at 222 nm will represent mainly the transition from the native to intermediate states, while neglecting the second transition to the denatured state.

The CD spectra of the intermediate and denatured states are not completely identical. At 200 nm, the denatured state ([V66L+G88V+G79S], pH 4.1, 90 °C) has approximately 50% more negative ellipticity than the intermediate state (54 °C, data not shown).

Table 1 also gives calorimetric data for four other mutant nucleases: L7A, E75G, G79S, and L137A. L7A and L137A, like A69T, show only very low second peaks, which we have not considered in the fitting of data. While L7A is classified as an m^- mutant (Green & Shortle, 1993), its m value of 0.89 makes it only weakly so. L137A is classified as m° ($0.9 \leq m \leq 1.1$) with an m value of 0.95 (Shortle et al., 1990). E75G and G79S proteins are both m^- (Green & Shortle, 1993) and clearly show second endotherms in the calorimeter. The E75G mutant has a much lower T_{t1} than either E75V (Carra et al., 1994c) or E75A (Table 1). The G79S mutant also is less stable than wild-type protein (T_{t1}, Table 2). The triple mutant [V66L+G88V+G79S] therefore contains two mutations which raise T_{t1} [V66L and G88V (Carra et al., 1994c)] and one which lowers T_{t1} (G79S). Our findings about the transition temperatures of these mutations, considering the first endotherm only, are similar to the previous calorimetric results of Tanaka et al. (1993).

The correlation we observe between the m^- characteristic and the presence of the thermal intermediate is strongly suggestive that solute-induced denaturation also occurs via a three-state mechanism for staphylococcal nuclease. Although calorimetry can supply a reliable test for the cooperativity of thermal unfolding (Privalov & Potekhin, 1986), for solute-induced denaturation there exists no definitive method to discriminate between two-state and multi-state mechanisms. If two transitions induced by guanidinium chloride are very well separated and the result biphasic, then a three-state mechanism is obvious. However, if the transitions partially overlap, then a multi-state process may superficially resemble a two-state process. While noncoincidence of curves obtained using different probes of melting can demonstrate the existence of an intermediate, coincidence of curves by itself cannot reliably prove a two-state mechanism. Ideally, whatever probes are used should reflect the complete folding process, but this is not always the case.

If we consider a three-state model, m^+ or m^- behavior would result from the respective destabilization or stabilization of an intermediate state versus the native state by mutations. Alternatively, in a two-state model, the m^- characteristic would reflect greater residual structure in the denatured state (Shortle & Meeker, 1986).

We have applied the transverse urea gradient gel electrophoresis method of Creighton (1979) to mutant nuclease proteins in an effort to discriminate between these hypotheses. m values for urea-induced denaturation of nuclease proteins are qualitatively similar to those for guanidinium chloride induced denaturation (Shortle & Meeker, 1986). The urea gradient gel method has the advantage of allowing comparison of the behavior of two or three proteins, including a wild-type reference, in the same experiment. It monitors changes in electrophoretic mobility, which may be taken as representing the time-averaged dimensions of the molecular population for each mutant protein. Figure 5A compares the denaturation of V23A, E75V (Carra et al., 1994c), and wild-type nucleases in a urea gradient gel. Panel

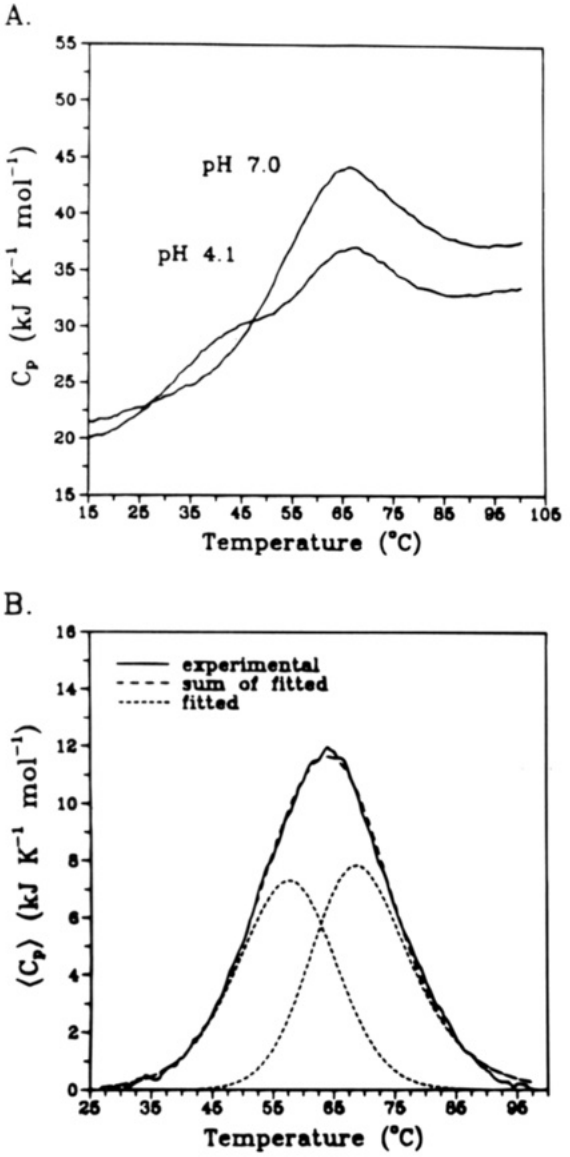

FIGURE 3: (A) DSC on the triple mutant protein [V66L+G88V+G79S] at pH 7.0 and pH 4.1. (B) The excess heat capacity function obtained for [V66L+G88V+G79S] at pH 7.0, showing the experimental result (—), the sum of the fitted curves (- - -), and the individual fitted transitions (▬).

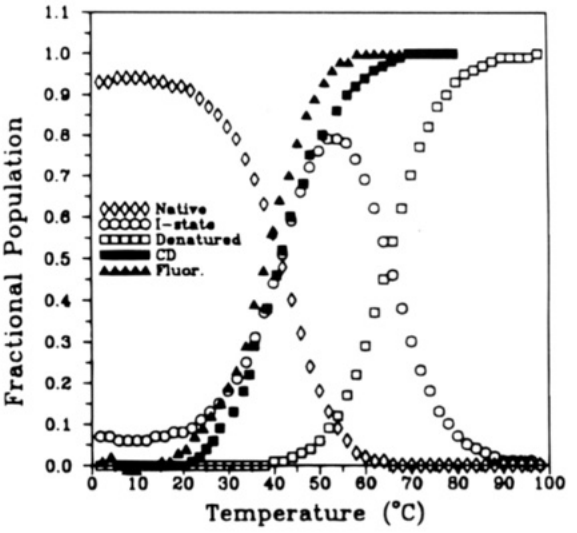

FIGURE 4: Population of states for the triple mutant [V66L+G88V+G79S] as a function of temperature at pH 4.1, calculated from the calorimetric data in Table 1, as previously described (Carra et al., 1994c). The fractional populations of the native state (◊), I-state (○), and denatured state (□) are shown, as well as the posttransitional population fractions found by circular dichroism at 222 nm (■), and by fluorescence from Trp_{140} (▲), also as described (Carra et al., 1994c).

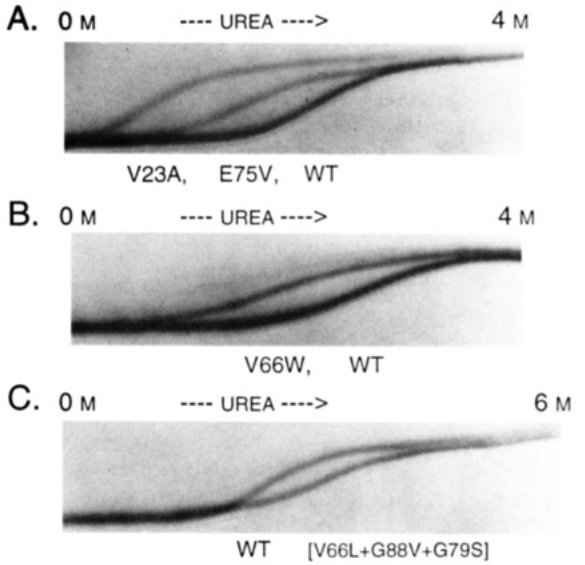

FIGURE 5: Transverse urea gradient gels. (A) 0−4 M urea gradient gel showing the denaturation of V23A, E75V, and wild-type nuclease proteins, as indicated on the figure. (B) 0−4 M urea gel with V66W and wild-type nucleases. (C) 0−6 M urea gel with wild-type and [V66L+G88V+G79S] nucleases.

5B shows wild-type and V66W (Carra et al., 1994c) proteins, and panel 5C shows wild-type and [V66L+G88V+G79S] proteins. The m^+ behavior of V23A and the m^- behavior of E75V, V66W, and [V66L+G88V+G79S] are apparent from the slope of the curve for each protein. The electrophoretic mobilities of the different proteins are not distinguishable from each other within the initial native and final denatured states.

The results of Figure 5 are most simply interpreted as showing broader denaturation through a three-state mechanism for the wild-type protein and the m^- mutants. While the thermal denaturation of the wild-type nuclease at pH 7.0 is essentially a two-state process (Griko et al., 1988; Carra et al., 1994a), this is not necessarily also true of solute-induced denaturation. The sharper transition of the m^+ mutant suggests its denaturation is more like a two-state process. Other interpretations of the results cannot be excluded, however. It is not possible from these data to rule out variations of a two-state mechanism for all the proteins, involving a first-order transition followed by a second-order transition occurring within a more loosely defined macroscopic denatured state (Dill & Shortle, 1991). The transverse urea gradient gel method has also been applied recently to nuclease mutants by Creighton and Shortle (1994).

It is questionable whether Gibbs free energies of protein folding can be obtained by the urea gel method for nuclease mutants, because this calculation must rely upon the two-state assumption. For example, backwards extrapolation of the data for [V66L+G88V+G79S] protein in Figure 5C to zero urea concentration would indicate that this mutant is less stable than the wild-type protein. This does not agree with its higher T_{tl} (Table 1), or its denaturation at higher urea concentrations (Figure 5C).

DISCUSSION

Two-State vs Three-State Models. We find that strong m^- mutants thermally denature via a three-state mechanism, while m^+ mutants follow a two-state mechanism. Therefore, we infer that the m^- characteristic results from the increased population of an intermediate state during guanidinium chloride denaturation. In other words, changes in the m value arise from changes in the cooperativity of folding. This conclusion suggests that the two-state assumption is invalid, and should not be applied, in any case where mutations are found to result in significant changes in the m value. This should apply not only to staphylococcal nuclease but also to mutational studies of other proteins such as lambda repressor (Lim et al., 1992), arc repressor (Milla et al., 1994), RNase T_1 (Pace et al., 1988), dihydrofolate reductase (Perry et al., 1989), and apomyoglobin (Hughson & Baldwin, 1989).

An analytical approach which defines the denatured state more loosely, including forms of substantial residual structure, has previously been applied to nuclease mutants (Green & Shortle, 1993; Shortle & Meeker, 1986; Shortle et al., 1990). Our interpretations differ crucially in that we use a narrower definition of denatured state, considering this residual structure as a discrete intermediate. Very different conclusions can be reached using these different reference systems. For example, using guanidinium chloride, fluorescence data, and the broadly defined two-state model, Shortle and Meeker (1986) calculated that the [V66L+G88V+G79S] mutant protein is 13 kJ mol^{-1} *less* stable than wild-type nuclease at 20 °C (Table 2). Our three-state analysis finds it to have a total Gibbs free energy of unfolding 3.2 kJ mol^{-1} *greater* than that of wild-type nuclease at 20 °C. Such a large difference in conclusions is obtained both because fluorescence from Trp_{140} monitors only the first endothermic transition (Figure 4) and because of the difference in reference state definition. Any analysis of the effects of mutations in terms of packing (Richards & Lim, 1994), hydrophobicity (Rose & Wolfenden, 1993), or other criteria must take into account the critical problem of reference states. Especially when the cooperativity, or mechanism, of unfolding changes, it is necessary to employ for all cases initial and final reference states which are the same, or as close as possible.

Sequence Specificity of the I-State. The structure present in the I-state appears to consist of the β-barrel portion of nuclease, judging from the results we presented in an earlier paper (Carra et al., 1994c), and the NMR structure of a nuclease fragment reported by Shortle and Abeygunawardana (1993). The β-barrel may usefully be considered as a subdomain of the protein, with the other subdomain being mainly α-helical. It is not entirely clear, however, if the structure of this part of the protein when it is in the intermediate state is exactly the same as when it is in the native state. Some resonances characteristic of the native β-barrel are not found in the NMR spectra of a nuclease fragment containing amino acids 1−136 and the mutation G88V (Shortle & Abeygunawardana, 1993). This suggests that the conformation of the intermediate is similar to the native fold, but more disordered.

A comparison of the results obtained from different substitutions at sites integral to the main hydrophobic core of the protein reveals that some amino acid substitutions are more readily tolerated by the intermediate state than others. Substitution of the buried valine at position 23 (Figure 1) by alanine gives an m^+ mutant (V23A), which thermally denatures via a two-state mechanism (Figure 2A). In contrast, substitution of a phenylalanine gives an m^- mutant (V23F), which denatures by a three-state mechanism (Figure 2B). In both cases, the mutation destabilizes the native state (T_{t1}, Table 1), but the phenylalanine is tolerated by the intermediate state while the alanine is not. Similar results are found for the buried valine at position 66, where an alanine substitution (V66A) is m^+ and does not show the thermal intermediate (Carra et al., 1993a), while a tryptophan substitution (V66W) is m^- and does yield the intermediate (Carra et al., 1994c; Gittis et al., 1993). We propose that it is precisely the differential effect of a mutation on the native versus intermediate states which determines if it is m^+ or m^-.

At both positions 23 and 66, the intermediate state discriminates against the smaller side chain of alanine, yet accommodates a larger aromatic amino acid. The native state is destabilized by all four substitutions. The amino acid *sequence specificity* of the intermediate state therefore can be said to be different from that of the native state [see Lattman and Rose (1993)]. This result would not be obtained if the structure present in the I-state were an exact subset of the native structure. A similar conclusion has been reached previously by a different line of reasoning (Shortle & Abeygunawardana, 1993). In contrast to the interpretations of Shortle and Abeygunawardana (1993), however, we find that mutations such as G88V and V66L, which raise T_{t1}, are stabilizing the structure in both the intermediate and the native states.

We can hypothesize that if the β-barrel core of nuclease is more disordered in the I-state, yet essentially intact, then substitutions of larger side chains may be accepted without great energetic cost from steric clashes. The more rigidly packed native state has less flexibility in adapting to the aromatic side chains. Smaller side chains such as alanine's methyl group have little volume and surface area to contribute to the core, and consequently the stabilities of the intermediate and native states are both lowered by alanine substitutions. A similar difference in sequence specificity has also been found between the native and I-states of apomyoglobin (Hughson & Baldwin, 1989; Hughson et al., 1991).

m^+ and m^- Mutations. m^+ behavior appears to result from mutational destabilization of the protein's hydrophobic core, which is still present in the intermediate state (Flanagan et al., 1993). m^- behavior is more complex and can be considered to arise from one of four different causes:

(1) Increased intrinsic stability of the β-barrel subdomain. The V66L and G88V mutations are examples.

(2) Decreased intrinsic stability of the α-helical subdomain. V111A, L125A, and L137G may be examples (Shortle et al., 1990).

(3) Loss of interactions maintaining cooperativity between subdomains. E75V, E75A, E75G, and D77A are examples [discussed in Carra et al. (1994c)].

(4) Differential destabilization of the native versus intermediate states at positions integral to the hydrophobic core. Examples are V66W and V23F.

Enthalpy of the Intermediate State. We have found that the effects of mutations on the enthalpy change of denaturation of staphylococcal nuclease are fairly small, as long as

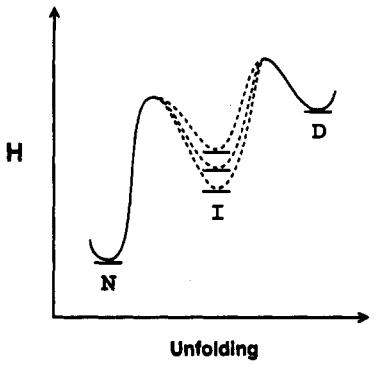

FIGURE 6: Energy diagram showing the enthalpy changes on going from the native (N) to intermediate (I) and to denatured (D) states. The intermediate state is shown as containing multiple enthalpic levels.

the enthalpy of the second transition of m^- mutants is included (Table 2). The changes in ΔH_{tot} observed are within the compounded error of measurement. If we compare the DSC curves for the K24G mutant and the E75A mutant (Figure 2A), for which T_{t1} is nearly equal, we can see that enthalpy lost from the first transition is shifted to the second transition. The amount of enthalpy present in the second transition is not the same, however, for all of the mutant proteins. The ΔH value of the second transition of the mutant [V66L+G88V+G79S] is twice that of E75A, E75G, G79S, or G88W (Table 1). The ΔH_{tot} of [V66L+G88V+G79S] is not greater than that of the other proteins (Table 2). Instead, more enthalpy has shifted from the first to the second transition. Circular dichroism results indicate that most or all of the α-helical content has been lost in the I-state of [V66L+G88V+G79S] protein (Figure 4), as with the single substitutions (Carra et al., 1994c). However, the greater enthalpy change of denaturation of the triple mutant's intermediate suggests that it has relatively more extent or cohesion of structure.

A smaller radius of gyration has been found by small-angle X-ray scattering for the nuclease fragment 1−136 when the [V66L+G88V+G79S] mutations are introduced, confirming an increase in compactness in that case (Flanagan et al., 1993). Melting of the 1−136 fragment is cooperative, and resembles the melting of the I-state observed with the complete protein (Griko et al., 1994b). Introduction of the G88V mutation into the 1−136 fragment causes more than 25 peaks in the $^{15}N-^{1}H$ proton correlation spectra to move away from random coil values (Shortle & Abeygunawardana, 1993), indicating a significant increase in structure.

The expected enthalpy difference between the native and intermediate states of a mutant nuclease has been calculated by Xie et al. (1994) from the protein structure, assuming that the β-barrel exists in the intermediate as an exact subset of the native state. The enthalpy difference predicted was significantly less than that obtained experimentally with the P117G mutant, which is comparable to the single mutant nucleases we have studied. Xie et al. attribute the difference between experimental and calculated results to looser packing of groups in the intermediate versus the native state. The small ΔH_1 value we find with the triple mutant [V66L+G88V+G79S] is more consistent with the enthalpy calculated for an exactly native β-barrel.

Figure 6 is a diagram of the enthalpy changes involved in unfolding through an intermediate state, considered at a temperature near 50 °C. The I-state is shown containing multiple enthalpic levels within the energy well which defines it as a separate state. The I-state of [V66L+G88V+G79S] protein would occupy one of the lower levels, because its ΔH_1 is relatively small and its ΔH_2 large. The high enthalpy barriers shown between the native, intermediate, and denatured states are justified by the observation of two first-order transitions. In the absence of a significant energy barrier between the I-state and denatured state, we would observe only a gradual non-cooperative melting of the intermediate, approximating the behavior of a second-order phase transition. This is expected to give only a broadly sloping change in the heat capacity function, not an actual peak, according to the analysis of Griko et al. (1994a) for apo-α-lactalbumin. The second peak observed here is well fit to a model two-state transition having a van't Hoff to calorimetric enthalpy ratio of 1 (Privalov & Potekhin, 1986), which is characteristic of a first-order phase transition.

Although the degree of structure present in the intermediate state of nuclease depends upon the amino acid sequence, what structure exists is highly cooperative in nature. Unfolding of the intermediate proceeds in an all-or-none way. In contrast, the cooperativity of residual structure in apo-α-lactalbumin at acidic pH is rather low, and unfolding proceeds gradually (Griko et al., 1994a). The inherent cooperativity of this intermediate state of staphylococcal nuclease encourages hope for the energetic decomposition of other small proteins into hierarchical structure elements, which are likely to represent kinetic intermediates on the pathway of protein folding.

ACKNOWLEDGMENT

We thank Drs. David Shortle and Alan Meeker for the gift of strains overproducing nuclease proteins, Dr. Ludwig Brand for the use of a fluorometer, Drs. Dong Xie and Ernesto Freire for communicating unpublished results, and Elizabeth Anderson for invaluable aid.

REFERENCES

Biltonen, R., & Freire, E. (1978) *Crit. Rev. Biochem. 5*, 85−124.
Calderon, R. O., Stolowich, N. J., Gerlt, J. A., & Sturtevant, J. M. (1985) *Biochemistry 24*, 6044−6049.
Carra, J., Anderson, E., & Privalov, P. (1994a) *Protein Sci. 3*, 944−951.
Carra, J., Anderson, E., & Privalov, P. (1994b) *Protein Sci. 3*, 952−959.
Carra, J., Anderson, E., & Privalov, P. (1994c) *Biochemistry 33*, 10842−10850.
Chen, H. M., & Tsong, T. Y. (1994) *Biophys. J. 66*, 40−45.
Creighton, T. (1979) *J. Mol. Biol. 129*, 235−264.
Creighton, T., & Shortle, D. (1994) *J. Mol. Biol. 242*, 670−682.
Dill, K. A., & Shortle, D. (1991) *Annu. Rev. Biochem. 60*, 795−825.
Flanagan, J., Kataoka, M., Fujisawa, T., & Engelman, D. (1993) *Biochemistry 32*, 10359−10370.
Gill, S., & von Hippel, P. (1989) *Anal. Biochem. 182*, 319−326.
Gittis, A., Stites, W., & Lattman, E. (1993) *J. Mol. Biol. 232*, 718−724.
Green, S., & Shortle, D. (1993) *Biochemistry 32*, 10131−10139.
Griko, Y., Privalov, P., Sturtevant, J., & Venyaminov, S. (1988) *Proc. Natl. Acad. Sci. U.S.A. 85*, 3343−3347.
Griko, Y., Freire, E., & Privalov, P. (1994a) *Biochemistry 33*, 1889−1899.
Griko, Y., Gittis, A., Lattman, E., & Privalov, P. (1994b) (in press).
Hughson, F., & Baldwin, R. (1989) *Biochemistry 28*, 4415−4422.
Hughson, F., Barrick, D., & Baldwin, R. (1991) *Biochemistry 30*, 4113−4118.

Jacobs, M., & Fox, R. (1994) *Proc. Natl. Acad. Sci. U.S.A. 91*, 449−453.
Kraulis, P. (1991) *J. App. Crystallogr. 24*, 946−950.
Lattman, E., & Rose, G. (1993) *Proc. Natl. Acad. Sci. U.S.A. 90*, 439−441.
Lim, W., Farruggio, D., & Sauer, R. (1992) *Biochemistry 31*, 4324−4333.
Loll, P., & Lattman, E. (1989) *Proteins: Struct., Funct., Genet. 5*, 183−201.
Makhatadze, G. I., & Privalov, P. L. (1990) *J. Mol. Biol. 213*, 375−384.
Makhatadze, G. I., & Privalov, P. L. (1993) *J. Mol. Biol. 232*, 639−659.
Milla, M., Brown, B., & Sauer, R. (1994) *Nature Struct. Biol. 1*, 518−523.
Pace, C., Grimsley, G., Thomson, J., & Barnett, B. (1988) *J. Biol. Chem. 263*, 11820−11825.
Perry, K., Onuffer, J., Gittelman, M., Barmat, L., & Matthews, C. (1989) *Biochemistry 28*, 7961−7968.
Privalov, P. L., & Potekhin, S. A. (1986) *Methods Enzymol. 131*, 4−51.
Privalov, P. L., & Makhatadze, G. I. (1993) *J. Mol. Biol. 232*, 660−679.
Richards, F., & Lim., W. (1994) *Q. Rev. Biophys. 26*, 423−498.
Rose, G., & Wolfenden, R. (1993) *Annu. Rev. Biophys. Biomol. Struct. 22*, 381−415.
Shortle, D., & Meeker, A. (1986) *Proteins: Struct., Funct., Genet. 1*, 81−89.
Shortle , D., & Abeygunawardana, C (1993) *Structure 1*, 121−134.
Shortle, D., Meeker, A., & Freire, E. (1988) *Biochemistry 27*, 4761−4768.
Shortle, D., Stites, W., & Meeker, A. (1990) *Biochemistry 29*, 8033−8041.
Sturtevant, J. (1994) *Curr. Opin. Struct. Biol. 4*, 69−78.
Tanaka, A., Flanagan, J., & Sturtevant, J. M. (1993) *Protein Sci. 2*, 567−576.
Wu, P., James, E., & Brand, L. (1994) *Biophys. Chem. 48*, 123−133.
Xie, D., Fox, R., & Freire, E. (1994) (in press).

BI942277F